

Generalized many-body exciton g-factors: magnetic hybridization and non-monotonic Rydberg series in monolayer WSe₂

Paulo E. Faria Junior,^{1,2,3,*} Daniel Hernangómez-Pérez,^{4,†}
Tomer Amit,^{5,‡} Jaroslav Fabian,³ and Sivan Refaelly-Abramson⁵

¹*Department of Physics, University of Central Florida, Orlando, Florida 32816, USA*

²*Department of Electrical and Computer Engineering,*

University of Central Florida, Orlando, Florida 32816, USA

³*Institute of Theoretical Physics, University of Regensburg, 93040 Regensburg, Germany*

⁴*CIC nanoGUNE BRTA, Tolosa Hiribidea 76, 20018 San Sebastián, Spain*

⁵*Department of Molecular Chemistry and Materials Science,
Weizmann Institute of Science, Rehovot 7610001, Israel*

Magneto-optics of low dimensional semiconductors, such as monolayer transition metal dichalcogenides, offers a vast playground for exploring complex quantum phenomena. However, current *ab initio* approaches fail to capture important experimental observations related to brightening of excitonic levels and their g-factor dependence. Here, we develop a robust and general first principles framework for many-body exciton g-factors by incorporating off-diagonal terms for the spin and orbital angular momenta of single-particle bands and many-body states for magnetic fields pointing in arbitrary spatial directions. We implement our framework using many-body perturbation theory via the GW-Bethe-Salpeter equation (BSE) and supplement our analysis with robust symmetry-based models, establishing a fruitful synergy between many-body GW-BSE and group theory. Focusing on the archetypal monolayer WSe₂, we accurately reproduce the known results of the low-energy excitons including the Zeeman splitting and the dark/grey exciton brightening. Furthermore, our theory naturally reveals fundamental physical mechanisms of magnetic-field hybridization of higher-energy excitons (s- and p-like) and resolves the long-standing puzzle of the experimentally measured non-monotonic Rydberg series (1s–4s) of exciton g-factors. Our framework offers a comprehensive approach to investigate, rationalize, and predict the non-trivial interplay between magnetic fields, angular momenta, and many-body exciton physics in van der Waals systems.

Introduction. Semiconducting transition metal dichalcogenides (TMDCs) are a family of two-dimensional, atomically thin layered van der Waals materials [1–5] that display unique electronic and optical properties, making them promising candidates for ultrathin optoelectronic, photovoltaic, and valleytronic applications [6–14]. Particularly, optical properties in TMDC systems are dominated by strongly bound excitons – quasiparticles resulting from the electron-hole Coulomb interaction [15–19]. For monolayers, the combination of broken inversion symmetry and strong spin-orbit interaction imprints selective coupling to circularly polarized light at the inequivalent K and –K points in the Brillouin zone[20, 21]. As a consequence, direct excitons display valley-dependent optical properties [22, 23]. Moreover, excitons carry intrinsic magnetic moments and effectively couple to external magnetic fields, revealing important effects such as many-body Zeeman shifts and magneto-optical selection rule modifications [24–47].

A fundamental framework for understanding magneto-exciton phenomena is provided by symmetry-based low-energy Hamiltonians [48, 49]. Such models explain why optically inactive (dark) excitons brighten under in-plane fields in TMDC monolayers due to spin-flip and valley-mixing terms [33, 50, 51]. However, a drawback of such approach is that these models do not offer quantitative insights into the coupling terms. Conversely, *ab initio* methods based on the many-body GW-Bethe-Salpeter

equation (BSE) [52–55] explicitly evaluate the underlying Coulomb interactions between the involved quantum states (conduction and valence bands), providing parameter-free information absent in purely symmetry-based models. In particular, the GW-BSE approach captures not only the spatial structure of the single-particle (Bloch) states but also of the excitonic states, achieved by explicitly considering the electron-hole basis and evaluating their many-body interactions. Within this formalism, the microscopic information about the crystal geometry, atomic nature, and orbital details of the wavefunctions can be incorporated perturbatively to calculate electronic and excitonic magnetic moments (g-factors) in TMDCs [38, 46, 56–58]. However, existing numerical evaluations of exciton g-factors remain incomplete by neglecting two critical aspects: (1) insights from group-theory analysis and (2) off-diagonal matrix elements (valley, orbital, and spin mixing) in the electronic and excitonic basis. These limitations severely hinder our ability to understand the fundamental aspects, such as spin-valley mixing, decoherence, and relaxation in realistic systems using reliable first principles techniques.

In this paper, we present a robust and general first-principles formalism to describe many-body exciton g-factors by incorporating off-diagonal elements of spin and orbital angular momenta, both in the single-particle and the exciton basis. These off-diagonal matrix elements are essential for capturing the correct spectral struc-

ture in degenerate many-body subspaces and therefore, exciton hybridization under arbitrarily oriented external magnetic fields. Our approach synergistically combines many-body perturbation theory within the GW-BSE framework with systematic symmetry-based analysis. We validate it by studying the exciton fine structure of monolayer WSe₂, a prototypical TMDC, reproducing the known results for the exciton Zeeman splitting, as well as the brightening dark/grey excitons in several magnetic field orientations [33, 50, 51]. Importantly, we demonstrate that off-diagonal angular momentum terms drive the brightening and hybridization of higher-energy excitons, including s-p mixing, and provide a natural resolution to the long-standing puzzle of the non-monotonic behavior in the excitonic Rydberg series g-factors (1s–4s) [36–39]. Our formalism opens new opportunities to investigate and predict the role of many-body effects on the non-trivial spin-valley physics of excitons in complex van der Waals systems.

General theory of exciton g-factors. The Hamiltonian describing two-particle excitations in the presence of an external magnetic field reads $\hat{H} = \hat{H}^{\text{BSE}} + \hat{\mathbf{g}} \cdot \mathbf{B}$ (further details in Sec. II of the Supplemental Material (SM) [59]). The term \hat{H}^{BSE} represents the BSE Hamiltonian, $\hat{\mathbf{g}} = (\hat{g}^x, \hat{g}^y, \hat{g}^z)$ corresponds to the g-factor, $\mathcal{B}_\epsilon := \mu_B B_\epsilon$, $B_{\epsilon=x,y,z}$ is the external magnetic field, and μ_B the Bohr magneton. In the exciton basis, the BSE Hamiltonian is diagonal, $\langle S | \hat{H}^{\text{BSE}} | S' \rangle = \Omega_S \delta_{S,S'}$ with Ω_S being the exciton energies. The magnetic coupling within degenerate and between different exciton subspaces is driven by the external magnetic field and characterized by the Hamiltonian matrix elements $\langle S | \hat{H} | S' \rangle = \sum_\epsilon g_{SS'}^\epsilon \mathcal{B}_\epsilon$, which are excitonic-dressed “generalized” g-factor matrix elements

$$g_{SS'}^\epsilon = \sum_{vck} (\mathcal{A}_{vc\mathbf{k}}^S)^* \left[\sum_{c'} \mathcal{A}_{vc'\mathbf{k}}^S g_{cc'\mathbf{k}}^\epsilon - \sum_{v'} \mathcal{A}_{v'c\mathbf{k}}^S g_{vv'\mathbf{k}}^\epsilon \right]. \quad (1)$$

Here, $g_{\alpha\alpha'\mathbf{k}}^\epsilon = \langle \alpha\mathbf{k} | \hat{L}^\epsilon + \hat{\Sigma}^\epsilon | \alpha'\mathbf{k} \rangle$ are the electronic g-factor matrix elements [60] accounting for the direct magnetic coupling, \hat{L}^ϵ ($\hat{\Sigma}^\epsilon$) the components of the orbital (spin) angular momentum operator in the Bloch basis, $|\alpha\mathbf{k}\rangle$, and $\mathcal{A}_{vc\mathbf{k}}^S$ the exciton amplitude obtained from the solution of the BSE. Eq. (1) extends on previous derivations [56, 57] by considering off-diagonal terms in the exciton g-factor, not only in the excitonic but also in the single-particle electron/hole manifold (band g-factors). For the latter, we need to consider off-diagonal matrix elements of single-particle operators in the Bloch basis. For instance, the orbital angular momentum in $\hat{\mathbf{z}}$ reads

$$L_{\alpha\alpha'\mathbf{k}}^z = \frac{1}{im_0} \left[\sum'_{\beta \neq \alpha} \frac{p_{\alpha\beta\mathbf{k}}^x p_{\beta\alpha'\mathbf{k}}^y - p_{\alpha\beta\mathbf{k}}^y p_{\beta\alpha'\mathbf{k}}^x}{\epsilon_{\alpha\mathbf{k}} - \epsilon_{\beta\mathbf{k}}} \right. \quad (2) \\ \left. - \sum'_{\beta \neq \alpha'} \frac{p_{\alpha\beta\mathbf{k}}^y p_{\beta\alpha'\mathbf{k}}^x - p_{\alpha\beta\mathbf{k}}^x p_{\beta\alpha'\mathbf{k}}^y}{\epsilon_{\alpha'\mathbf{k}} - \epsilon_{\beta\mathbf{k}}} \right]$$

with $p_{\alpha\beta\mathbf{k}}^\epsilon = \langle \alpha\mathbf{k} | \hat{p}^\epsilon | \beta\mathbf{k} \rangle$ [61], i being the imaginary unit, and m_0 the bare electron mass. The $'$ in the first (second) summation indicates that the α' (α) state must be excluded if α and α' are in the same degenerate subset.

Low-energy excitons. We demonstrate our theoretical approach for the archetypal monolayer WSe₂, extensively studied via magneto-optics [28, 33, 36–40, 50, 51, 62, 63]. The top view of the TMDC crystals (D_{3h} symmetry group) and the first Brillouin zone are depicted in Figs. 1(a,b), respectively. We focus on the subspace of low-energy excitons visible in typical magneto-photoluminescence experiments. These excitons arise from the top valence band, VB_+ , and the lowest conduction bands, CB_\pm , in the vicinity of the K-valleys. In Fig. 1(c) we show VB_+ and CB_\pm , highlighting their irreducible representations (*irreps*) and the direction of

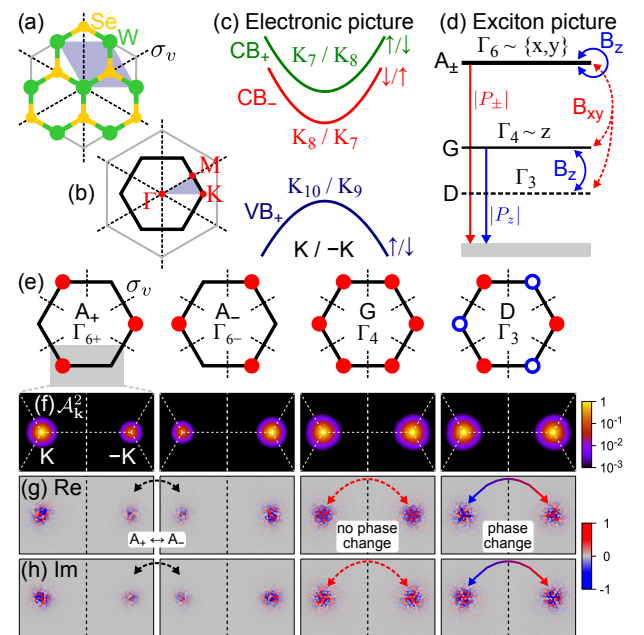


Figure 1. (a) Top view of the monolayer WSe₂. The colored parallelogram indicates the primitive unit cell. (b) First Brillouin zone. The colored triangle indicates the irreducible wedge. The dashed lines in panels (a,b) indicate the mirror planes σ_v . (c) Low-energy bands at K – K valleys, including the irreps and spin orientation. (d) Low-energy exciton states at the Γ -point, identified by their labeling and irreps (see main text). Vertical arrows indicate the allowed optical transitions. Curved arrows indicate couplings via the magnetic field (solid for $\mathbf{B} \parallel z$ and dashed for $\mathbf{B} \parallel x, y$). (e) Schematic representation of the exciton wavefunctions. Closed (open) circles indicate positive (negative) amplitudes. For irrep Γ_6 , the subindex $+(-)$ refers to the exciton wavefunction mainly localized in the $+(-)K$ -valley. (f) Absolute, (g) real, and (h) imaginary values of the calculated GW-BSE exciton wavefunctions. The arrows in panels (g,h) emphasize the effect of σ_v , i. e., $\Gamma_{6+}(A_+) \leftrightarrow \Gamma_{6-}(A_-)$, no phase change for Γ_4 (G), and phase change for Γ_3 (D).

the spin expectation value in the out-of-plane direction (Σ^z) at $\pm\mathbf{K}$ valleys (C_{3h} point group with complex double group irreps). The interband optical selection rules at $\pm\mathbf{K}$ can be readily evaluated within group theory (see Sec. III of the SM [59]), revealing that the transitions $\text{CB}_- \rightarrow \text{VB}_+ \sim K_4$ are optically active with z polarization at $\pm\mathbf{K}$ points, while $\text{CB}_+ \rightarrow \text{VB}_+ \sim K_3(K_2)$ are optically active with s_+ (s_-) polarization at \mathbf{K} ($-\mathbf{K}$) point, in agreement with previous results [21, 64, 65]. Here, we adopt the group theory nomenclature of Ref. 66.

To evaluate the irreps of the direct (1s-like) excitons, we map the irreps from the \mathbf{K} -valleys to the Γ -point. Using the compatibility relations ($C_{3h} \rightarrow D_{3h}$), we find $K_2 \oplus K_3 \rightarrow \Gamma_6$ and $K_4 \rightarrow \Gamma_3/\Gamma_4$, with $\Gamma_6 \sim x, y$ and $\Gamma_4 \sim z$. The two possibilities of mapping K_4 to Γ_3 or Γ_4 arise from their distinct behavior under the mirror plane σ_v operation, identified in Figs. 1(a,b), as a consequence of the intervalley exchange coupling [33, 64, 67]. We employ the typical nomenclature for these excitons [33, 50, 51]: bright ($A \sim \Gamma_6$), grey ($G \sim \Gamma_4$), and dark ($D \sim \Gamma_3$). From the symmetry perspective, A excitons are two-fold degenerate while the D exciton has zero oscillator strength. The resulting low-energy subspace, optical selection rules, and coupling to an external \mathbf{B} -field are summarized in Fig. 1(d), with the schematic representation of the exciton wavefunctions given in Fig. 1(e).

Our GW-BSE calculations provide the exciton energies and oscillator strengths (Table II in the SM [59]), supplying a clear identification of these 4 exciton states. Notably, the symmetry analysis also allows us to identify the numerical precision of the GW-BSE calculations. The energy values (oscillator strengths) fully satisfy the symmetry constraints up to 0.1 meV ($10^{-3} e^2 a_0^2$). The exciton energy splitting between G and A excitons is ~ 52.4 meV while the D - G exciton splitting is ~ 2.4 meV, in excellent agreement with experimental observations in hBN encapsulated samples [33, 50, 51, 65]. One relevant aspect of the numerical effects in the GW-BSE calculations is the mixing of the A exciton states, *i.e.*, the two states do not emit light with completely circular polarization. This is a common effect in first-principles calculations whenever the irreps are (nearly) numerically degenerate [68, 69]. To verify the features from Fig. 1(e) at the GW-BSE level, we display in Figs. 1(f-h) the density ($\rho_{\mathbf{k}}^S = \sum_{vc} |\mathcal{A}_{vc\mathbf{k}}^S|^2$), real ($\text{Re}\{\mathcal{A}_{\mathbf{k}}^S\} = \sum_{vc} \text{Re}\{\mathcal{A}_{vc\mathbf{k}}^S\}$), and imaginary ($\text{Im}\{\mathcal{A}_{\mathbf{k}}^S\} = \sum_{vc} \text{Im}\{\mathcal{A}_{vc\mathbf{k}}^S\}$) values of the computed *ab initio* exciton wavefunctions. Because of the numerical degeneracy in the A exciton subspace, the wavefunctions are not fully localized in $\pm\mathbf{K}$ but are still connected by the mirror plane σ_v . For the G and D excitons, the sign change is visible in the real and imaginary parts, evidenced by the dashed (G) and solid (D) arrows.

Knowing the excitons' symmetry allows us to incorporate the effect of external magnetic fields, which transform as pseudovector objects ($B_{x,y} \sim \Gamma_5$ and $B_z \sim \Gamma_2$).

The resulting symmetry-allowed couplings in the low-energy excitons are shown in Fig. 1(d), revealing that out-of-plane fields ($\mathbf{B} \parallel z$) yield Zeeman splitting physics for the A exciton subset and mixing of D and G excitons, while in-plane fields ($\mathbf{B} \parallel x, y$) introduce exciton mixing between A and D/G states. We emphasize here the relevance of our general formalism: mixing effects can only be captured by off-diagonal matrix elements, which are also relevant for degenerate subsets such as the A exciton. The details of the symmetry analysis and connection to the microscopic contributions of electron g-factors in the exciton basis are given in Sec. III of the SM [59]. We incorporate the magnetic field within GW-BSE by numerically evaluating Eq. (1), including the \mathbf{k} -space extension of the exciton wavefunctions coupled via the full matrices Σ and L .

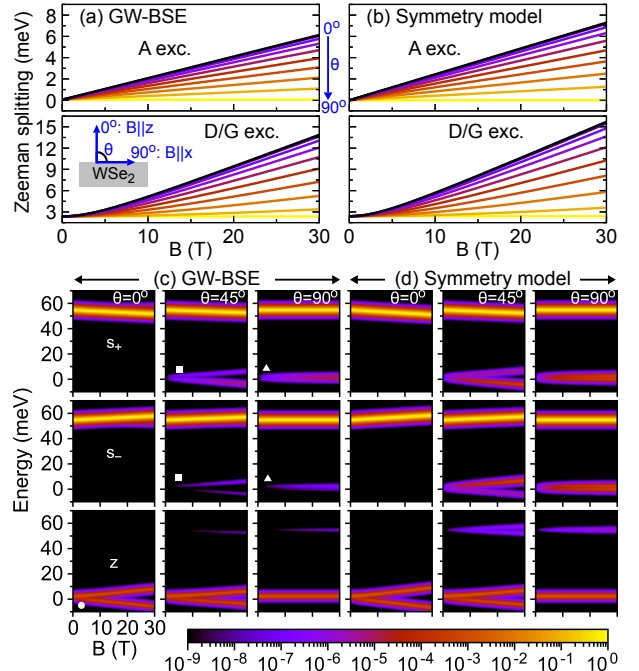


Figure 2. Zeeman splitting of the low-energy excitons under applied magnetic field at different angles, θ , for (a) the GW-BSE and (b) the symmetry-adapted model. The top (bottom) panels correspond to the A (D/G) excitons. Calculated absorption via the (c) GW-BSE and (d) symmetry-adapted model under applied magnetic field oriented at different angles ($\theta = 0^\circ, 45^\circ, 90^\circ$) for s_+ (top row), s_- (middle row), and z (bottom row) polarizations. The spectra are normalized to the maximum value of the s_+ emission. For each transition, a broadening was applied using a sech function with 1 meV full-width at half-maximum. The closed circle, squares, and triangles highlight important brightening signatures.

To validate our approach, we show in Figs. 2(a-b) the Zeeman splitting of A and D/G excitons for different orientations of the magnetic field. In the symmetry model we assume δ -like exciton wavefunctions fully localized at

$\pm K$ points, as in previous works [51]. Besides the difference in the Zeeman splitting (~ 1.2 meV at 30 T, due to the \mathbf{k} -space exciton wavefunction spread [46, 56, 57]), all the dependencies match accordingly, revealing that the exciton couplings are properly captured by our general *ab initio* formalism.

The magneto-optical signature of exciton mixing is observed in the intensity of the photoluminescence spectra [33, 50, 51]. In Figs. 2(c-d) we present the calculated absorption spectra in logarithmic scale [70] for different magnetic field orientations ($\theta = 0^\circ, 45^\circ, 90^\circ$). Our calculations reproduce all the relevant mixing-induced brightening mechanisms observed experimentally: (1) brightening of the D exciton due to the D-G mixing for out-of-plane fields [33] (closed circle); (2) brightening of both G and D excitons in tilted magnetic fields [50] (squares); and (3) brightening of both D and G excitons for in-plane fields [51] (triangles). The mixing-induced exciton brightening under magnetic fields is a direct consequence of the off-diagonal elements of the spin and orbital angular momenta matrices, correctly incorporated in the general expression, Eq. (1), of the exciton g-factor.

Magnetic-hybridization of high-energy excitons. While low-energy excitons are easily described by effective models, high-energy excitons (often called *excited* excitons) pose a greater challenge due to the increasingly denser excitonic manifold of available states with enhanced intervalley exchange and spin-orbital mixing. To emphasize the significance of the exciton hybridization at higher energies, we present in Fig. 3(a-b) the absolute values of the out-of-plane and in-plane g-factors for the lowest 20 excitons (see Sec. V of the SM [59] for a larger exciton subset). Notably, both g-factor components display significant presence of off-diagonal elements responsible for hybridizing states that belong to different exciton subspaces, completely absent in previous studies [56, 57]. Moreover, g-factors of p-like excitons (indices 5-12 and 17-20) have similar magnitude of their s-like counterparts (indices 1-4 and 12-16). In Sec. V of the SM [59] we present the exciton wavefunctions.

In Fig. 3(c-e) we display the calculated absorption for s_{\pm} and z polarization for the exciton subset shown in Fig. 3(a-b). For s_{\pm} polarizations, external magnetic fields lead to the brightening of several optically inactive excitonic states. In particular, we reveal a clear signature of the mixing of s-p excitons, recently observed by external in-plane electric fields in monolayer WSe₂ [71]. For z-polarized light, we recover the brightening of the excited D/G states, see Fig. 2(c). Similar to the recently proposed s-p mixing of excitons in van der Waals heterostructures [72], this brightening cannot be captured by purely (Wannier or symmetry-based) effective models, underscoring the importance of including the full complexity of the excitonic spectrum using the generalized GW-BSE treatment.

Rydberg series of g-factors. To showcase the robust ca-

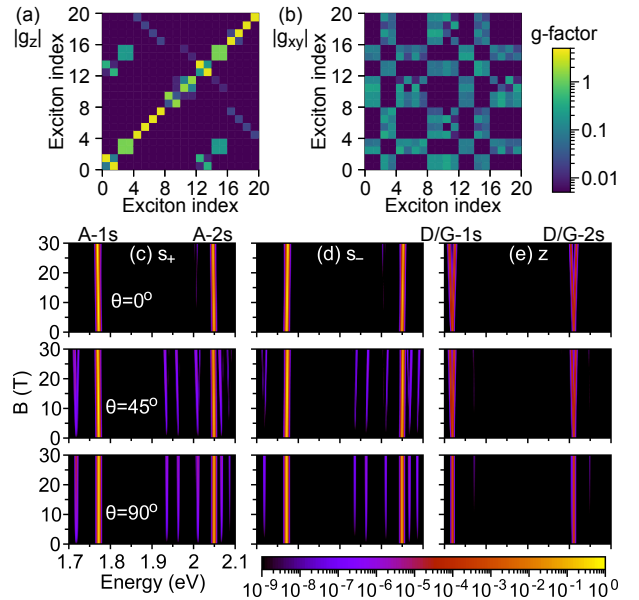


Figure 3. Absolute value of the (a) out-of-plane g-factor matrix, g_z , and (b) in-plane g-factor matrix, $|g_{xy}| = \sqrt{g_x^2 + g_y^2}$, via Eq. (1), as a function of the exciton index, demonstrating the significance of the off-diagonal terms. Calculated absorption for high-energy excitons as a function of the magnetic field oriented at different angles ($\theta = 0^\circ, 45^\circ, 90^\circ$) using the GW-BSE approach for (c) s_+ , (d) s_- , and (e) z polarizations. The values are normalized to the maximum value of the s_+ emission. We apply the same broadening as in Fig. 2. Several exciton peaks emerge around 1.95 eV, visible for $\theta = 45^\circ, 90^\circ$. We consider the nonzero oscillator strengths only for s-like exciton states.

pabilities of our approach, we address the long-standing puzzle and conflicting experimental reports of the Rydberg series of the A exciton g-factors for the so-called 1s-4s states. Fig. 4(a) compiles the available experimental g-factors in hBN-encapsulated monolayer WSe₂ from Refs. [36–39]. These experiments reveal an overall decreasing trend together with clear non-monotonic signatures, varying slightly due to environmental and sample-dependent factors [73–75].

In Fig. 4(b), we present our calculated g-factors via the full *ab initio* GW-BSE approach, revealing that non-monotonic features naturally emerge from our formalism (see Sec. V of the SM [59] for the wavefunctions of 1s-4s states). Notably, the g-factors for D/G Rydberg excitons also exhibit non-monotonic dependencies, see inset of Fig. 4(b). We also evaluate the g-factors using an effective (parabolic) two-band model incorporating the dielectric screening of vacuum and hBN-encapsulation (see Sec. I of the SM [59]). The effective model systematically yields a monotonic behavior and fails to reproduce the oscillations obtained in the GW-BSE g-factor calculations via Eq. (1). These non-monotonic features cannot be explained by simplified models but naturally emerge from

our generalized GW-BSE formalism, which incorporates orbital and spin mixing induced by external magnetic fields. Our results firmly indicate that the interplay between the excitonic fine structure and magnetic response is highly nontrivial and strongly dependent on the exciton state, emphasizing the need for first-principles-based approaches when interpreting high-resolution magneto-optical measurements.

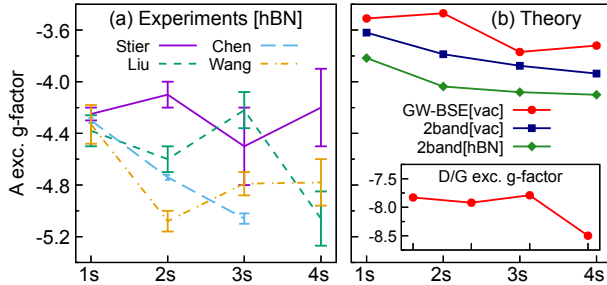


Figure 4. (a) Experimental g-factors of the Rydberg series (1s–4s) of the A exciton by Stier *et al.* [36], Liu *et al.* [37], Chen *et al.* [38], and Wang *et al.* [39]. (a) Calculated g-factors via the GW-BSE approach (circles), using an effective two-band model (squares), and via the two-band model considering hBN encapsulation (diamonds). Notably, the observed non-monotonic trends can only be accurately reproduced using our *ab initio* GW-BSE generalized g-factor theory. Inset: g-factors of D/G Rydberg excitons, also exhibiting non-monotonic features.

Conclusions. In this paper, we developed a robust and general framework based on *ab initio* many-body GW-BSE formalism that incorporates the interplay of the spin and orbital angular momenta via the exciton g-factors. This approach takes into account the hybridization of single-particle bands and many-body states through off-diagonal matrix elements of spin and orbital angular momenta. Moreover, we establish a previously-unexplored synergy between GW-BSE and group theory models of excitonic subspaces. We validate our approach for the archetypal TMDC monolayer WSe₂, capturing and rationalizing the observed results of the exciton Zeeman splitting as well as brightening of the optically dark/grey excitons by in-plane/tilted magnetic fields. We also explore the brightening of high-energy excitons, a challenging task for pure symmetry-based models, emphasizing that many-body off-diagonal components of the g-factor are crucial to capture the magnetic mixing of exciton states. These results imply that interpreting high-energy features in magneto-optics requires caution, as nominally distinct excitonic subspaces can strongly hybridize. Furthermore, the robustness of our approach allows us to unveil the non-monotonic behavior of the Rydberg series of exciton g-factors, a long-standing puzzle observed by several experimental groups [36–39]. Our novel approach provides a robust foundation to study many-body

effects of multidirectional magneto-excitons in other complex two-dimensional materials and van der Waals heterostructures. It is particularly relevant to study non-trivial spin-valley dynamics [76] and unusual topological and chiral excitons [77, 78] as well as many-body effects in the emergent field of orbitronics [79].

The authors acknowledge the financial support of the Deutsche Forschungsgemeinschaft (DFG, German Research Foundation) SFB 1277 (Project No. 314695032) and the European Research Council (ERC) Starting Grant No. 101041159. P.E.F.J. acknowledges the computational resources of the Advanced Research Computing Center of the University of Central Florida. D. H.-P. acknowledges the funding from the Diputación Foral de Gipuzkoa through Grants 2023-FELL-000002-01, 2024-FELL-000009-01, from the Spanish MICIU/AEI/10.13039/501100011033 and FEDER, UE through Project No. PID2023-147324NA-I00, and the computational resources of the Max Planck Computing and Data Facility (MPCDF) cluster. T.A. acknowledges support from the Azrieli Graduate Fellows Program.

* These authors contributed equally; corresponding authors: paulo@ucf.edu

† These authors contributed equally; corresponding author: d.hernangomez@nanogune.eu

‡ These authors contributed equally.

- [1] Q. H. Wang, K. Kalantar-Zadeh, A. Kis, J. N. Coleman, and M. S. Strano, Electronics and optoelectronics of two-dimensional transition metal dichalcogenides, *Nat. Nanotechnol.* **7**, 699 (2012).
- [2] A. K. Geim and I. V. Grigorieva, Van der Waals heterostructures, *Nature* **499**, 419 (2013).
- [3] K. S. Novoselov, A. Mishchenko, A. Carvalho, and A. H. C. Neto, 2D materials and van der Waals heterostructures, *Science* **353**, aac9439 (2016).
- [4] Y. Liu, N. O. Weiss, X. Duan, H.-C. Cheng, Y. Huang, and X. Duan, Van der Waals heterostructures and devices, *Nat. Rev. Mater.* **1**, 16042 (2016).
- [5] S. Manzeli, D. Ovchinnikov, D. Pasquier, O. V. Yazyev, and A. Kis, 2D transition metal dichalcogenides, *Nat. Rev. Mater.* **2**, 17033 (2017).
- [6] B. Radisavljevic, A. Radenovic, J. Brivio, V. Giacometti, and A. Kis, Single-layer MoS₂ transistors, *Nat. Nanotechnol.* **6**, 147 (2011).
- [7] O. López-Sánchez, D. Lembke, M. Kayci, A. Radenovic, and A. Kis, Ultrasensitive photodetectors based on monolayer MoS₂, *Nat. Nanotechnol.* **8**, 497 (2013).
- [8] D. Jariwala, V. K. Sangwan, L. J. Lauhon, T. J. Marks, and M. C. Hersam, Emerging device applications for semiconducting two-dimensional transition metal dichalcogenides, *ACS Nano* **8**, 1102 (2014).
- [9] A. Pospischil, M. M. M. Furchi, and T. Mueller, Solar-energy conversion and light emission in an atomic monolayer p–n diode, *Nat. Nanotechnol.* **9**, 257 (2014).
- [10] F. Withers, O. Del Pozo-Zamudio, A. Mishchenko, A. P.

- Rooney, A. Gholinia, K. Watanabe, T. Taniguchi, S. J. Haigh, A. K. Geim, A. I. Tartakovskii, and K. S. Novoselov, Light-emitting diodes by band-structure engineering in van der Waals heterostructures, *Nat. Mater.* **14**, 301 (2015).
- [11] J. R. Schaibley, H. Yu, G. Clark, P. Rivera, J. S. Ross, K. L. Seyler, W. Yao, and X. Xu, Valleytronics in 2D materials, *Nat. Rev. Mater.* **1**, 16055 (2016).
- [12] Z. Ye, D. Sun, and T. F. Heinz, Optical manipulation of valley pseudospin, *Nat. Phys.* **13**, 26 (2017).
- [13] K. F. Mak and J. Shan, Photonics and optoelectronics of 2D semiconductor transition metal dichalcogenides, *Nat. Photonics* **10**, 216 (2016).
- [14] K. F. Mak, D. Xiao, and J. Shan, Light–valley interactions in 2D semiconductors, *Nat. Photonics* **12**, 451 (2018).
- [15] K. F. Mak, C. Lee, J. Hone, J. Shan, and T. F. Heinz, Atomically thin MoS₂: A new direct-gap semiconductor, *Phys. Rev. Lett.* **105**, 136805 (2010).
- [16] A. Splendiani, L. Sun, Y. Zhang, T. Li, J. Kim, C.-Y. Chim, G. Galli, and F. Wang, Emerging photoluminescence in monolayer MoS₂, *Nano Lett.* **10**, 1271 (2010).
- [17] D. Y. Qiu, F. H. da Jornada, and S. G. Louie, Optical spectrum of MoS₂: Many-body effects and diversity of exciton states, *Phys. Rev. Lett.* **111**, 216805 (2013).
- [18] A. Chernikov, T. C. Berkelbach, H. M. Hill, A. Rigosi, Y. Li, B. Aslan, D. R. Reichman, M. S. Hybertsen, and T. F. Heinz, Exciton binding energy and nonhydrogenic rydberg series in monolayer WS₂, *Phys. Rev. Lett.* **113**, 076802 (2014).
- [19] G. Wang, A. Chernikov, M. M. Glazov, T. F. Heinz, X. Marie, T. Amand, and B. Urbaszek, Colloquium: Excitons in atomically thin transition metal dichalcogenides, *Rev. Mod. Phys.* **90**, 021001 (2018).
- [20] T. Cao, G. Wang, W. Han, H. Ye, C. Zhu, J. Shi, Q. Niu, P. Tan, E. Wang, B. Liu, and J. Feng, Valley-selective circular dichroism of monolayer molybdenum disulphide, *Nat. Commun.* **3**, 887 (2012).
- [21] D. Xiao, G.-B. Liu, W. Feng, X. Xu, and W. Yao, Coupled spin and valley physics in monolayers of MoS₂ and other group-VI dichalcogenides, *Phys. Rev. Lett.* **108**, 196802 (2012).
- [22] G. Sallen, L. Bouet, X. Marie, G. Wang, C. R. Zhu, W. P. Han, Y. Lu, P. H. Tan, T. Amand, B. L. Liu, and B. Urbaszek, Robust optical emission polarization in MoS₂ monolayers through selective valley excitation, *Phys. Rev. B* **86**, 081301 (2012).
- [23] K. F. Mak, K. He, J. Shan, and T. F. Heinz, Control of valley polarization in monolayer MoS₂ by optical helicity, *Nat. Nanotechnol.* **7**, 494 (2012).
- [24] Y. Li, J. Ludwig, T. Low, A. Chernikov, X. Cui, G. Arefe, Y. D. Kim, A. M. van der Zande, A. Rigosi, H. M. Hill, S. H. Kim, J. Hone, Z. Li, D. Smirnov, and T. F. Heinz, Valley splitting and polarization by the Zeeman effect in monolayer MoSe₂, *Phys. Rev. Lett.* **113**, 266804 (2014).
- [25] D. MacNeill, C. Heikes, K. F. Mak, Z. Anderson, A. Kormányos, V. Zólyomi, J. Park, and D. C. Ralph, Breaking of valley degeneracy by magnetic field in monolayer MoSe₂, *Phys. Rev. Lett.* **114**, 037401 (2015).
- [26] G. Wang, L. Bouet, M. Glazov, T. Amand, E. Ivchenko, E. Palleau, X. Marie, and B. Urbaszek, Magneto-optics in transition metal diselenide monolayers, *2D Mater.* **2**, 034002 (2015).
- [27] A. Srivastava, M. Sidler, A. V. Allain, D. S. Lembke, A. Kis, and A. İmamoğlu, Valley Zeeman effect in elementary optical excitations of monolayer WSe₂, *Nat. Phys.* **11**, 141 (2015).
- [28] G. Aivazian, Z. Gong, A. M. Jones, R.-L. Chu, J. Yan, D. G. Mandrus, C. Zhang, D. Cobden, W. Yao, and X. Xu, Magnetic control of valley pseudospin in monolayer WSe₂, *Nat. Phys.* **11**, 148 (2015).
- [29] A. Mitioglu, P. Plochocka, Á. Granados del Aguila, P. Christianen, G. Deligeorgis, S. Anghel, L. Kulyuk, and D. Maude, Optical investigation of monolayer and bulk tungsten diselenide (WSe₂) in high magnetic fields, *Nano Lett.* **15**, 4387 (2015).
- [30] A. V. Stier, K. M. McCreary, B. T. Jonker, J. Kono, and S. A. Crooker, Exciton diamagnetic shifts and valley Zeeman effects in monolayer WS₂ and MoS₂ to 65 tesla, *Nat. Commun.* **7**, 10643 (2016).
- [31] A. V. Stier, N. P. Wilson, G. Clark, X. Xu, and S. A. Crooker, Probing the influence of dielectric environment on excitons in monolayer WSe₂: insight from high magnetic fields, *Nano Lett.* **16**, 7054 (2016).
- [32] R. Schmidt, A. Arora, G. Plechinger, P. Nagler, A. Granados del Águila, M. V. Ballottin, P. C. M. Christianen, S. Michaelis de Vasconcellos, C. Schüller, T. Korn, and R. Bratschitsch, Magnetic-field-induced rotation of polarized light emission from monolayer WS₂, *Phys. Rev. Lett.* **117**, 077402 (2016).
- [33] C. Robert, T. Amand, F. Cadiz, D. Lagarde, E. Courtade, M. Manca, T. Taniguchi, K. Watanabe, B. Urbaszek, and X. Marie, Fine structure and lifetime of dark excitons in transition metal dichalcogenide monolayers, *Phys. Rev. B* **96**, 155423 (2017).
- [34] X.-X. Zhang, T. Cao, Z. Lu, Y.-C. Lin, F. Zhang, Y. Wang, Z. Li, J. C. Hone, J. A. Robinson, D. Smirnov, S. G. Louie, and T. F. Heinz, Magnetic brightening and control of dark excitons in monolayer WSe₂, *Nat. Nanotech.* **12**, 883 (2017).
- [35] A. Arora, M. Koperski, A. Slobodeniuk, K. Nogajewski, R. Schmidt, R. Schneider, M. R. Molas, S. M. de Vasconcellos, R. Bratschitsch, and M. Potemski, Zeeman spectroscopy of excitons and hybridization of electronic states in few-layer WSe₂, MoSe₂ and MoTe₂, *2D Mater.* **6**, 015010 (2018).
- [36] A. V. Stier, N. P. Wilson, K. A. Velizhanin, J. Kono, X. Xu, and S. A. Crooker, Magnetooptics of exciton rydberg states in a monolayer semiconductor, *Phys. Rev. Lett.* **120**, 057405 (2018).
- [37] E. Liu, J. van Baren, T. Taniguchi, K. Watanabe, Y.-C. Chang, and C. H. Lui, Magnetophotoluminescence of exciton Rydberg states in monolayer WSe₂, *Phys. Rev. B* **99**, 205420 (2019).
- [38] S.-Y. Chen, Z. Lu, T. Goldstein, J. Tong, A. Chaves, J. Kunstmänn, L. S. R. Cavalcante, T. Woźniak, G. Seifert, D. R. Reichman, T. Taniguchi, K. Watanabe, D. Smirnov, and J. Yan, Luminescent emission of excited rydberg excitons from monolayer WSe₂, *Nano Lett.* **19**, 2464 (2019).
- [39] T. Wang, Z. Li, Y. Li, Z. Lu, S. Miao, Z. Lian, Y. Meng, M. Blei, T. Taniguchi, K. Watanabe, S. Tongay, D. Smirnov, C. Zhang, and S.-F. Shi, Giant valley-polarized Rydberg excitons in monolayer WSe₂ revealed by magneto-photocurrent spectroscopy, *Nano Lett.* **20**, 7635 (2020).

- [40] C. Robert, H. Dery, L. Ren, D. Van Tuan, E. Courtade, M. Yang, B. Urbaszek, D. Lagarde, K. Watanabe, T. Taniguchi, T. Amand, and X. Marie, Measurement of conduction and valence bands g -factors in a transition metal dichalcogenide monolayer, *Phys. Rev. Lett.* **126**, 067403 (2021).
- [41] M. Zinkiewicz, T. Woźniak, T. Kazimierczuk, P. Kapuscinski, K. Oreszczuk, M. Grzeszczyk, M. Bartoś, K. Nogajewski, K. Watanabe, T. Taniguchi, C. Faugeras, P. Kossacki, M. Potemski, A. Babiński, and M. R. Molas, Excitonic complexes in n-doped WS₂ monolayer, *Nano Lett.* **21**, 2519 (2021).
- [42] A. Arora, Magneto-optics of layered two-dimensional semiconductors and heterostructures: Progress and prospects, *J. Appl. Phys.* **129**, 120902 (2021).
- [43] P. E. Faria Junior, K. Zollner, T. Woźniak, M. Kurpas, M. Gmitra, and J. Fabian, First-principles insights into the spin-valley physics of strained transition metal dichalcogenides monolayers, *New J. Phys.* **24**, 083004 (2022).
- [44] F. S. Covre, P. E. Faria Junior, V. O. Gordo, C. S. de Brito, Y. V. Zhumagulov, M. D. Teodoro, O. D. D. Couto, L. Misoguti, S. Pratavieira, M. B. Andrade, P. C. M. Christianen, J. Fabian, F. Withers, and Y. Galvão Gobato, Revealing the impact of strain in the optical properties of bubbles in monolayer MoSe₂, *Nanoscale* **14**, 5758 (2022).
- [45] E. Blundo, P. E. Faria Junior, A. Surrente, G. Pettinari, M. A. Prosnikov, K. Olkowska-Pucko, K. Zollner, T. Woźniak, A. Chaves, T. Kazimierczuk, M. Fellici, A. Babiński, M. R. Molas, P. C. M. Christianen, J. Fabian, and A. Polimeni, Strain-induced exciton hybridization in WS₂ monolayers unveiled by Zeeman-splitting measurements, *Phys. Rev. Lett.* **129**, 067402 (2022).
- [46] P. E. Faria Junior, T. Naimer, K. M. McCreary, B. T. Jonker, J. J. Finley, S. A. Crooker, J. Fabian, and A. V. Stier, Proximity-enhanced valley Zeeman splitting at the WS₂/graphene interface, *2D Mater.* **10**, 034002 (2023).
- [47] K. Olkowska-Pucko, T. Woźniak, E. Blundo, N. Zawadzka, Lucja Kipczak, P. E. Faria Junior, J. Szpakowski, G. Krasucki, S. Cianci, D. Vaclavkova, D. Jana, P. Kapuściński, M. Grzeszczyk, D. Cecchetti, G. Pettinari, I. Antoniazzi, Z. Sofer, I. Plutnarová, K. Watanabe, T. Taniguchi, C. Faugeras, M. Potemski, A. Babiński, A. Polimeni, and M. R. Molas, Extremely high excitonic g -factors in 2D crystals by alloy-induced admixing of band states, *arXiv:2503.23071* (2025).
- [48] K. Cho, Unified theory of symmetry-breaking effects on excitons in cubic and wurtzite structures, *Phys. Rev. B* **14**, 4463 (1976).
- [49] H. Venghaus, S. Suga, and K. Cho, Magnetoluminescence and magnetoreflectance of the A exciton of CdS and CdSe, *Phys. Rev. B* **16**, 4419 (1977).
- [50] M. R. Molas, C. Faugeras, A. O. Slobodeniu, K. Nogajewski, M. Bartos, D. M. Basko, and M. Potemski, Brightening of dark excitons in monolayers of semiconducting transition metal dichalcogenides, *2D Mater.* **4**, 021003 (2017).
- [51] M. R. Molas, A. O. Slobodeniu, T. Kazimierczuk, K. Nogajewski, M. Bartos, P. Kapuściński, K. Oreszczuk, K. Watanabe, T. Taniguchi, C. Faugeras, P. Kossacki, D. M. Basko, and M. Potemski, Probing and manipulating valley coherence of dark excitons in monolayer WSe₂, *Phys. Rev. Lett.* **123**, 096803 (2019).
- [52] M. S. Hybertsen and S. G. Louie, Electron correlation in semiconductors and insulators: Band gaps and quasi-particle energies, *Phys. Rev. B* **34**, 5390 (1986).
- [53] M. Rohlfing and S. G. Louie, Electron-hole excitations in semiconductors and insulators, *Phys. Rev. Lett.* **81**, 2312 (1998).
- [54] S. Albrecht, L. Reining, R. Del Sole, and G. Onida, Ab initio calculation of excitonic effects in the optical spectra of semiconductors, *Phys. Rev. Lett.* **80**, 4510 (1998).
- [55] X. Blase, I. Duchemin, D. Jacquemin, and P.-F. Loos, The Bethe-Salpeter equation formalism: From physics to chemistry, *J. Phys. Chem. Lett.* **11**, 7371 (2020).
- [56] T. Deilmann, P. Krüger, and M. Rohlfing, Ab initio studies of exciton g factors: Monolayer transition metal dichalcogenides in magnetic fields, *Phys. Rev. Lett.* **124**, 226402 (2020).
- [57] T. Amit, D. Hernangómez-Pérez, G. Cohen, D. Y. Qiu, and S. Refaelly-Abramson, Tunable magneto-optical properties in MoS₂ via defect-induced exciton transitions, *Phys. Rev. B* **106**, L161407 (2022).
- [58] L. Kipczak, A. O. Slobodeniu, T. Woźniak, M. Bhattacharjee, N. Zawadzka, K. O. Pucko, M. J. Grzeszczyk, K. Watanabe, T. Taniguchi, A. Babinski, and M. Molas, Analogy and dissimilarity of excitons in monolayer and bilayer of MoSe₂, *2D Mater.* **1**, 025014 (2023).
- [59] See Supplemental Material at URL for the computational details, the representation of spin and orbital operators in the excitonic basis, the symmetry analysis, additional computational data, and additional figures. It also contains Refs. [33, 43, 46, 50–53, 56–58, 66, 68, 69, 80–106].
- [60] In this form, the g -factor is simply the total angular momentum, $\mathbf{J} = \mathbf{L} + \mathbf{S}$ with spin-orbit effects incorporated via the basis functions.
- [61] Non-local effects in the band g -factors [107, 108] are not considered. We focus on the combined effect of the excitonic properties within nearly-degenerate subspaces.
- [62] M. Koperski, K. Nogajewski, A. Arora, V. Cherkez, P. Mallet, J.-Y. Veuillet, J. Marcus, P. Kossacki, and M. Potemski, Single photon emitters in exfoliated WSe₂ structures, *Nat. Nanotech.* **10**, 503 (2015).
- [63] K.-Q. Lin, C. S. Ong, S. Bange, P. E. Faria Junior, B. Peng, J. D. Ziegler, J. Zipfel, C. Bäuml, N. Paradiso, K. Watanabe, T. Taniguchi, C. Strunk, B. Monserrat, J. Fabian, A. Chernikov, D. Y. Qiu, S. G. Louie, and J. M. Lupton, Narrow-band high-lying excitons with negative-mass electrons in monolayer WSe₂, *Nat. Commun.* **12**, 5500 (2021).
- [64] H. Dery and Y. Song, Polarization analysis of excitons in monolayer and bilayer transition-metal dichalcogenides, *Phys. Rev. B* **92**, 125431 (2015).
- [65] G. Wang, C. Robert, M. M. Glazov, F. Cadiz, E. Courtade, T. Amand, D. Lagarde, T. Taniguchi, K. Watanabe, B. Urbaszek, and X. Marie, In-plane propagation of light in transition metal dichalcogenide monolayers: Optical selection rules, *Phys. Rev. Lett.* **119**, 047401 (2017).
- [66] G. F. Koster, J. O. Dimmock, R. G. Wheeler, and H. Statz, *Properties of the thirty-two point groups*, Vol. 24 (MIT press, 1963).
- [67] M. M. Glazov, T. Amand, X. Marie, D. Lagarde,

- L. Bouet, and B. Urbaszek, Exciton fine structure and spin decoherence in monolayers of transition metal dichalcogenides, *Phys. Rev. B* **89**, 201302 (2014).
- [68] J. V. V. Cassiano, A. de Lelis Araújo, P. E. Faria Junior, and G. J. Ferreira, Dft2kp: Effective kp models from ab initio data, *SciPost Physics Codebases* **25**, 10.21468/scipostphyscodeb.25 (2024).
- [69] S. Zhang, H. Sheng, Z.-D. Song, C. Liang, Y. Jiang, S. Sun, Q. Wu, H. Weng, Z. Fang, X. Dai, *et al.*, Vasp2kp: k-p models and Landé g-factors from ab initio calculations, *Chin. Phys. Lett.* **40**, 127101 (2023).
- [70] In photoluminescence experiments, the optical spectra incorporate the optical selection rules and the exciton occupation (Boltzmann distribution function [109] with rapid exponential decay). Therefore, the emission of A, G, and D excitons display similar intensities [33, 50, 51, 63, 110], which can also influenced by the aperture of the objective lens used to collect the emitted light [63].
- [71] B. Zhu, K. Xiao, S. Yang, K. Watanabe, T. Taniguchi, and X. Cui, In-plane electric-field-induced orbital hybridization of excitonic states in monolayer WSe₂, *Phys. Rev. Lett.* **131**, 036901 (2023).
- [72] J. D. Cao, K. S. Denisov, and I. Zutic, Tunable resonant s-p mixing of excitons in van der Waals heterostructures, [arXiv:2503.11927](https://arxiv.org/abs/2503.11927) (2025).
- [73] L. Mennel, M. M. Furchi, S. Wachter, M. Paur, D. K. Polyushkin, and T. Mueller, Optical imaging of strain in two-dimensional crystals, *Nat. Commun.* **9**, 516 (2018).
- [74] A. Raja, L. Waldecker, J. Zipfel, Y. Cho, S. Brem, J. D. Ziegler, M. Kulig, T. Taniguchi, K. Watanabe, E. Malic, T. F. Heinz, T. C. Berkelsbach, and A. Chernikov, Dielectric disorder in two-dimensional materials, *Nat. Nanotech.* **14**, 832 (2019).
- [75] P. V. Kolesnichenko, Q. Zhang, T. Yun, C. Zheng, M. S. Fuhrer, and J. A. Davis, Disentangling the effects of doping, strain and disorder in monolayer WS₂ by optical spectroscopy, *2D Mater.* **7**, 025008 (2020).
- [76] S. Raiber, P. E. Faria Junior, D. Falter, S. Feldl, P. Marzena, K. Watanabe, T. Taniguchi, J. Fabian, and C. Schüller, Ultrafast pseudospin quantum beats in multilayer WSe₂ and MoSe₂, *Nat. Commun.* **13**, 4997 (2022).
- [77] B. Hou, D. Wang, B. A. Barker, and D. Y. Qiu, Exchange-driven intermixing of bulk and topological surface states by chiral excitons in bi₂se₃, *Phys. Rev. Lett.* **130**, 216402 (2023).
- [78] H.-Y. Xie, P. Ghaemi, M. Mitrano, and B. Uchoa, Theory of topological exciton insulators and condensates in flat chern bands, *PNAS* **121**, e2401644121 (2024).
- [79] T. P. Cysne, L. M. Canonico, M. Costa, R. B. Muniz, and T. G. Rappoport, Orbitronics in two-dimensional materials, [arXiv:2502.12339](https://arxiv.org/abs/2502.12339) (2025).
- [80] W. Schutte, J. De Boer, and F. Jellinek, Crystal structures of tungsten disulfide and diselenide, *J. Solid State Chem.* **70**, 207 (1987).
- [81] M. Camarasa-Gómez, A. Ramasubramaniam, J. B. Neaton, and L. Kronik, Transferable screened range-separated hybrid functionals for electronic and optical properties of van der Waals materials, *Phys. Rev. Mater.* **7**, 104001 (2023).
- [82] P. Giannozzi, S. Baroni, N. Bonini, M. Calandra, R. Car, C. Cavazzoni, D. Ceresoli, G. L. Chiarotti, M. Cococcioni, I. Dabo, A. Dal Corso, S. de Gironcoli, S. Fabris, G. Fratesi, R. Gebauer, U. Gerstmann, C. Gougaud, A. Kokalj, M. Lazzeri, L. Martin-Samos, N. Marzari, F. Mauri, R. Mazzarello, S. Paolini, A. Pasquarello, L. Paulatto, C. Sbraccia, S. Scandolo, G. Sclauzero, A. P. Seitsonen, A. Smogunov, P. Umari, and R. M. Wentzcovitch, QUANTUM ESPRESSO: a modular and open-source software project for quantum simulations of materials, *J. Phys. Condens. Matter* **21**, 395502 (2009).
- [83] P. Giannozzi, O. Andreussi, T. Brumme, O. Bunau, M. Buongiorno Nardelli, M. Calandra, R. Car, C. Cavazzoni, D. Ceresoli, M. Cococcioni, N. Colonna, I. Carnimeo, A. Dal Corso, S. de Gironcoli, P. Delugas, R. A. DiStasio, A. Ferretti, A. Floris, G. Fratesi, G. Fugallo, R. Gebauer, U. Gerstmann, F. Giustino, T. Gorni, J. Jia, M. Kawamura, H.-Y. Ko, A. Kokalj, E. Küçükbenli, M. Lazzeri, M. Marsili, N. Marzari, F. Mauri, N. L. Nguyen, H.-V. Nguyen, A. Otero-de-la Roza, L. Paulatto, S. Poncé, D. Rocca, R. Sabatini, B. Santra, M. Schlipf, A. P. Seitsonen, A. Smogunov, I. Timrov, T. Thonhauser, P. Umari, N. Vast, X. Wu, and S. Baroni, Advanced capabilities for materials modelling with Quantum ESPRESSO, *J. Phys. Condens. Matter* **29**, 465901 (2017).
- [84] P. Giannozzi, O. Baseggio, P. Bonfà, D. Brunato, R. Car, I. Carnimeo, C. Cavazzoni, S. de Gironcoli, P. Delugas, F. Ferrari Ruffino, A. Ferretti, N. Marzari, I. Timrov, A. Urru, and S. Baroni, Quantum ESPRESSO toward the exascale, *J. Chem. Phys.* **152**, 154105 (2020).
- [85] J. P. Perdew, K. Burke, and M. Ernzerhof, Generalized gradient approximation made simple, *Phys. Rev. Lett.* **77**, 3865 (1996).
- [86] M. J. van Setten, M. Giantomassi, E. Bousquet, M. J. Verstraete, D. R. Hamann, X. Gonze, and G.-M. Rignanese, The pseudodojo: Training and grading a 85 element optimized norm-conserving pseudopotential table, *Comput. Phys. Commun.* **226**, 39 (2018).
- [87] P. Blaha, K. Schwarz, F. Tran, R. Laskowski, G. K. Madsen, and L. D. Marks, Wien2k: An APW+lo program for calculating the properties of solids, *J. Chem. Phys.* **152**, 074101 (2020).
- [88] K. Lejaeghere, G. Bihlmayer, T. Björkman, P. Blaha, S. Blügel, V. Blum, D. Caliste, I. E. Castelli, S. J. Clark, A. D. Corso, S. de Gironcoli, T. Deutsch, J. K. Dewhurst, I. D. Marco, C. Draxl, M. Dułak, O. Eriksson, J. A. Flores-Livas, K. F. Garrity, L. Genovese, P. Giannozzi, M. Giantomassi, S. Goedecker, X. Gonze, O. Gränäs, E. K. U. Gross, A. Gulans, F. Gygi, D. R. Hamann, P. J. Hasnip, N. A. W. Holzwarth, D. Iuşan, D. B. Jochym, F. Jollet, D. Jones, G. Kresse, K. Koepernik, E. Küçükbenli, Y. O. Kvashnin, I. L. M. Locht, S. Lubeck, M. Marsman, N. Marzari, U. Nitzsche, L. Nordström, T. Ozaki, L. Paulatto, C. J. Pickard, W. Poelmans, M. I. J. Probert, K. Refson, M. Richter, G.-M. Rignanese, S. Saha, M. Scheffler, M. Schlipf, K. Schwarz, S. Sharma, F. Tavazza, P. Thunström, A. Tkatchenko, M. Torrent, D. Vanderbilt, M. J. van Setten, V. V. Speybroeck, J. M. Wills, J. R. Yates, G.-X. Zhang, and S. Cottenier, Reproducibility in density functional theory calculations of solids, *Science* **351**, aad3000 (2016).
- [89] D. J. Singh and L. Nordstrom, *Planewaves, Pseudopotentials, and the LAPW method* (Springer Science & Business Media, 2006).

- [90] J. Deslippe, G. Samsonidze, D. A. Strubbe, M. Jain, M. L. Cohen, and S. G. Louie, BerkeleyGW: A massively parallel computer package for the calculation of the quasiparticle and optical properties of materials and nanostructures, *Comput. Phys. Commun.* **183**, 1269 (2012).
- [91] M. Rohlffing and S. G. Louie, Electron-hole excitations and optical spectra from first principles, *Phys. Rev. B* **62**, 4927 (2000).
- [92] M. Wu, *Spin-Orbit Coupling, Broken Time-Reversal Symmetry, and Polarizability Self-Consistency in GW and GW-BSE Theory with Applications to Two-Dimensional Materials*, Ph.D. thesis, University of California, Berkeley (2020).
- [93] B. A. Barker, J. Deslippe, J. Lischner, M. Jain, O. V. Yazyev, D. A. Strubbe, and S. G. Louie, Spinor GW/Bethe-Salpeter calculations in BerkeleyGW: Implementation, symmetries, benchmarking, and performance, *Phys. Rev. B* **106**, 115127 (2022).
- [94] F. H. da Jornada, D. Y. Qiu, and S. G. Louie, Nonuniform sampling schemes of the Brillouin zone for many-electron perturbation-theory calculations in reduced dimensionality, *Phys. Rev. B* **95**, 035109 (2017).
- [95] S. Ismail-Beigi, Truncation of periodic image interactions for confined systems, *Phys. Rev. B* **73**, 233103 (2006).
- [96] T. Woźniak, P. E. Faria Junior, G. Seifert, A. Chaves, and J. Kunstmann, Exciton *g*-factors of van der Waals heterostructures from first-principles calculations, *Phys. Rev. B* **101**, 235408 (2020).
- [97] N. S. Rytova, Screened potential of a point charge in a thin film, *Moscow University Physics Bulletin* **3**, 30 (1967).
- [98] L. V. Keldysh, Coulomb interaction in thin semiconductor and semimetal films, *JETP Lett.* **29**, 658 (1979).
- [99] A. Laturia, M. L. Van de Put, and W. G. Vandenberghe, Dielectric properties of hexagonal boron nitride and transition metal dichalcogenides: from monolayer to bulk, *npj 2D Mater. Appl.* **2**, 6 (2018).
- [100] Y. G. Gobato, C. S. de Brito, A. Chaves, M. A. Prosnikov, T. Woźniak, S. Guo, I. D. Barcelos, M. V. Milošević, F. Withers, and P. C. M. Christianen, Distinctive *g*-factor of moiré-confined excitons in van der Waals heterostructures, *Nano Lett.* **22**, 8641 (2022).
- [101] M. Kurpas, M. Gmitra, and J. Fabian, Spin-orbit coupling and spin relaxation in phosphorene: Intrinsic versus extrinsic effects, *Phys. Rev. B* **94**, 155423 (2016).
- [102] M. Kurpas, P. E. Faria Junior, M. Gmitra, and J. Fabian, Spin-orbit coupling in elemental two-dimensional materials, *Phys. Rev. B* **100**, 125422 (2019).
- [103] Y. Yafet, *g* factors and spin-lattice relaxation of conduction electrons, in *Solid state physics*, Vol. 14 (Elsevier, 1963).
- [104] S. Bhowal and G. Vignale, Orbital hall effect as an alternative to valley hall effect in gapped graphene, *Phys. Rev. B* **103**, 195309 (2021).
- [105] A. Urru, O. P. O. Ivo Souza, S. S. Tsirkin, and D. Vanderbilt, Optical spatial dispersion via wannier interpolation, *arXiv:2504.09742* (2025).
- [106] J. J. Esteve-Paredes, M. A. García-Blázquez, A. J. Uría-Alvarez, M. Camarasa-Gómez, and J. J. Palacios, Excitons in nonlinear optical responses: shift current in MoS₂ and GeS monolayers, *npj Comput. Mater.* **11**, 13 (2025).
- [107] F. Xuan and S. Y. Quek, Valley Zeeman effect and Landau levels in two-dimensional transition metal dichalcogenides, *Phys. Rev. Res.* **2**, 033256 (2020).
- [108] F. Xuan and S. Y. Quek, Valley-filling instability and critical magnetic field for interaction-enhanced Zeeman response in doped WSe₂ monolayers, *npj Comput. Mater.* **7**, 198 (2021).
- [109] Y. V. Zhumagulov, A. Vagov, D. R. Gulevich, P. E. Faria Junior, and V. Perebeinos, Trion induced photoluminescence of a doped MoS₂ monolayer, *J. Chem. Phys.* **153**, 044132 (2020).
- [110] F. Dirnberger, J. D. Ziegler, P. E. Faria Junior, R. Bushati, T. Taniguchi, K. Watanabe, J. Fabian, D. Bougeard, A. Chernikov, and V. M. Menon, Quasi-1D exciton channels in strain-engineered 2D materials, *Sci. Adv.* **7**, eabj3066 (2021).